

## DIAGNOSTIC OF THE BEHAVIOUR OF A COURSE-CORRECTION AMMUNITION DURING ITS CORRECTION PHASE

A. Ziliani<sup>1</sup>, C. Grignon<sup>1</sup>, C. Trouillot<sup>1</sup>, C. Jeannin<sup>2</sup>

<sup>1</sup> *Giat Industries, 7 route de Guerry, 18023 Bourges Cédex, France*

<sup>2</sup> *ETBS, Carrefour de Zéro-Nord, Route de Guerry, B.P. 712, 18015 Bourges Cédex, France*

Future ammunitions have to be more and more accurate. One way to decrease the range error is to use a correction fuze increasing the aerodynamic drag in a well defined flight scenario. The GPS correction fuze SAMPRASS has been developed in conjunction with Giat Industries, TDA and Sextant Avionique under DGA contract. The study presented in this paper deals with an aeroballistic analysis based on wind tunnel tests, flight tests and complementary aspects relative to the behaviour of a projectile fitted with the SAMPRASS fuze (opening conditions of the airbrakes, security, ...)

### PRINCIPLE OF THE COURSE-CORRECTION

The course-correction system is integrated in the SAMPRASS<sup>1</sup> fuze. It is made of three drag brakes radially disposed so that the angles between two neighbours is 120° (Fig. 1). The increase of the aerodynamic drag produced by the well timed opening of the three airbrakes leads to a reduction of the range error of the artillery projectile. This fuze screws on to the front part of the projectile in place of a classical fuze.

The projectile is fired with an elevation angle corresponding to a virtual impact located behind the target. The GPS data received by the fuze is relayed to a ground processor near the weapon which command-deploys the drag brakes at the appropriate point of the trajectory (Fig. 2). The opening function is ensured by a pyrotechnical device. As the center of gravity of each airbrake is not located on the inertial longitudinal axis of the projectile, the translatory motion of the airbrake can occur under the action of the centrifugal acceleration.

<sup>1</sup> Système d'AMélioration de la PRécision de l'Artillerie Sol-Sol

## WIND TUNNEL TESTS

Wind tunnel tests have been carried out in the ONERA<sup>2</sup> S3MA blow-down pressurized sub/trans and supersonic wind tunnel situated in Modane-Avrieux (France) to characterize projectile aerodynamics.

The main test conditions are given below:

Static coefficients	CA,CN,Cm
Mach numbers	0.6 ; 0.9 ; 1.2 ; 1.35 ; 1.5 ; 1.8 ; 2.1
Dynamic coefficients	CY (Cypα),Cn (Cnpα)
Mach numbers	0.6 ; 0.9 ; 1.35 ; 1.5 ; 1.86 ; 2.12
Reynolds number range	[0.73.10 <sup>6</sup> ; 4.44.40 <sup>6</sup> ]
Stagnation pressure (bars)	[1.1 ; 2.7]
Angle of attack range (°)	[0 ; 18]
Spin rate range (RPM)	[0 ; 24000]

Experimental program, S3MA wind tunnel, ONERA.

The static and dynamic forces and moments are measured by the mean of a 6 or 4 component sting type strain gauge balance. Note that a boundary layer trip was placed on the ogive to force a reliable turbulent flow. In order to observe the flow, the Schlieren visualization technique was used.

Then, before the flight tests, a complete system analysis can be done (to study the efficiency of the airbrakes in terms of range error reduction for example, security aspects, ...) or more phenomenological descriptions (static and dynamic stabilities, ...). For example, from a security point of view, it is interesting to study the sensitivity of a partial or untimely opening on the behaviour of the projectile. To do it, aerodynamic asymmetries have been tested in the S3MA wind tunnel. Kinematics of the opening can also be taken into account in order to study the influence of the force generated by the brutally stopped displacement of each airbrake on the behaviour of the projectile.

Opening tests have also been carried out in the wind tunnel in order to study the opening under the action of the dynamic pressure occurring on the airbrakes orthogonally to their translatory motion. Combination between spin rate (linked to the centrifugal acceleration responsible for the translatory motion) and the Mach number (linked to the dynamic pressure inducing a resistance force to the translatory motion) have been investigated. It has been demonstrated that the action of the dynamic pressure won't, nor prevent the translatory motion of the airbrakes neither produce a permanent deformation induced by the buckling effect.

Fig. 3 and 4 show the supersonic flow developed around the projectile with and without the correction fuze. The "screen effect" induced by the airbrakes is clearly illustrated. The increase of drag, presented in terms of drag coefficient  $C_x$  on Fig. 5, directly expressed the efficiency of the correction fuze. It is interesting to note that the difference is not the same in the subsonic and in the supersonic flight. In fact, the efficiency of the correction (that is the  $C_x$  ratio between the two configurations) would be more important in the subsonic part. For a "classical" projectile, it is known that the maximum value of  $C_x$

<sup>2</sup> Office National d'Etudes et de Recherches Aéropatiales

at zero angle of attack (noted  $C_{x0}$ ) is reached for Mach  $\sim 1.05$ . The tests show that the maximum value of  $C_{x0}$  for the projectile fitted with the correction fuze is reached for a superior Mach number. This has already been observed for full ring airbrakes for example used for vertical flights [1].

## **FLIGHT TESTS**

The SAMPRASS concept has been evaluated in real flight. Evaluation has been carried out at the DGA/ETBS<sup>3</sup> field of fire in Bourges (France) in the following conditions:

- 155 mm howitzer, 39 caliber long, AUF1 type
- 155 mm OGR F1 ammunition fitted with the SAMPRASS fuze
- elevation angle:  $27^\circ$
- range reduction by comparing the corrected shot to a non-corrected one in the same conditions: 850 m
- opening time of the airbrakes: 25.8 s
- radar and optronic turrets trackings
- aerological measurements

The trajectory and the projectile behaviour have been simulated by the mean of a 6 degrees of freedom (dof) model with the aerodynamic coefficients determined by the wind tunnel tests. The aim was to consolidate the aerodynamic database concerning the projectile fit out with SAMPRASS in real flight conditions by 6 dof inverse analysis and to evaluate its efficiency in real conditions.

### **Radial velocity and acceleration**

The comparison between the removal velocity measured by the radar and determined by the model shows a good agreement (Fig. 6). This velocity is based on the distance separating the projectile from its initial position. The slope increase (in terms of absolute value) occurring at 25.8 s corresponds to the braking effect when the projectile leaves its purely ballistic flight to enter the corrected phase. The removal acceleration shows clearly as well this change in flight (Fig. 7). We can notice the step in the removal acceleration occurring near 18 s which corresponds to the transsonic region of the non corrected phase through which the drag coefficient brutally decreases (Fig. 5 and 8).

## Trajectory

Measured and simulated trajectories can be compared (Fig. 9 and 10) in order to ensure that the theoretical expected trajectory is really the one obtained experimentally without global or local unexpected phenomenon. The fact that the wind came from the right hand side has produced an opposition to the natural deviation to the right due to the gyroscopic effect (Fig. 12).

## Behaviour of the projectile in flight

The simulated angular motion in flight conditions (Fig. 13) shows oscillations of the total angle of attack  $\delta$  representing the angle between the projectile longitudinal axis and its instantaneous velocity vector. It is interesting to eliminate wind effects to understand the origins of the oscillations without this exterior disturbing source. Figure 14 shows oscillations when the projectile leaves the barrel (no other aerodynamic jump is added to introduce fluttering at the expulsion). These natural oscillations vanish well before the opening of the airbrakes occurs. As the polar diagram shows, the projectile rapidly flies very close to its sideslip plan (in that case, the sideslip angle  $\beta$  is equivalent to  $\delta$ ). Let note that the angle  $\psi$  mentioned on Fig. 13 and 14 represents the angle between the vertical plan containing the velocity vector and the resistance plan containing the longitudinal axis of the projectile and its velocity.

The opening under significant angle of attack conditions produces a supplementary aerodynamic moment (due to the important change in the drag force) whose damping occurs in the correction phase as the second oscillating motion shows it. The combination between spin and yaw/pitch motions produces spirals in the polar diagram. The comparison between Fig. 13 and 14 shows the consequences of wind on the angular motion and demonstrates that the increase of the total angle of attack at the end of the correction phase is due to sheared wind layers at low altitudes (Fig. 12) and not, for example, to stability problems. This important variation of the side wind between the ground and a 2000 m altitude is responsible for the fact that the flight has difficulties to occur in the sideslip plan of the projectile (this is only illustrating the disturbing effect of wind on the behaviour and, consequently, on the trajectory of a projectile, which are the base of the general problem of accuracy of non-guided artillery projectiles). As Fig. 10 shows it, this also justifies the increase of the left deviation just before the impact (the projectile is exposed to a rather high intensity side wind coming from the right).

## PERCUSSION DUE TO THE OPENING OF THE AIRBRAKES

It is difficult to quantify the disturbances induced by the impact of the airbrakes at the end of their translatory motion when they are stopped by a mechanical thrust. The following study probably simplifies reality and, for example, avoids all the dynamic mechanical phenomena involved in the impact (the total duration of the opening is a few milliseconds). The kinematic decomposition shows that the first airbrake moves and liberates

the second one before the end of its translatory motion. The second liberates the third and last one before the end of the second translatory motion. So three impacts occur and might induce a rocking motion of the projectile. A simple approach would consist in considering that the force generated by the centrifugal acceleration due to ends of translatory motions of airbrakes is totally converted into the rocking acceleration. The mass of airbrakes being very small, this approach leads to insignificant disturbances (a few decirad/s).

Considering that dynamic phenomena have been avoided, let us consider two disturbance levels (i.e. two rocking rates) which appear to be excessive for this kind of problem: 2 and 5 rad/s. 6 dof simulations with these supplementary disturbances show a small influence on the impact, even if disturbances are excessive (Fig. 15). The roll angle being parametric, the impacts constitute a flattened contour. Fig. 15 shows that the effect of roll angle only induces a very small lateral distribution of the impacts. The range loss obtained, even with a demonstrative 5 rad/s disturbance level, doesn't exceed 7 m! To conclude, nor aerodynamic neither mechanical shock occurring when airbrakes open seems to affect the ground impact position.

## **PARTIAL OPENING OF THE AIRBRAKES**

The study of the consequences of a partial opening is interesting for security aspects. The opening sequence of each airbrake has been introduced in the 6 dof model. Let us take into account the opening of one airbrake or two airbrakes at the good time in order to examine the lateral dispersion. The simulation results show that the aerodynamic asymmetry due to a partial opening has weak consequences on lateral dispersion. This can be explained by the smoothing effect due to spin which makes that, for one complete spin turn, the asymmetry effect is practically cancelled (Fig. 16).

## **CONCLUSION**

Aeroballistic aspects concerning a projectile fitted with the correction fuze SAM-PRASS has been presented. Wind tunnel tests show a good efficiency level in terms of drag increase during the course-correction phase. Flight tests have also been investigated and demonstrated the efficiency of the device. An inverse 6 dof analysis has allowed to consolidate to aerodynamic behaviour of the projectile previously examined in wind tunnel tests. As a complement, consequences of a partial opening of the airbrakes on the dispersion of the impact (security aspects) have been studied and have shown that the lateral dispersion was very weak. The percussion effect produced by the end of the opening of the airbrakes on the behaviour of the projectile has also been investigated and has demonstrated that, even for excessive disturbances levels, the projectile remains stable and the dispersion of the impacts on the ground was not significant.

## **ACKNOWLEDGEMENTS**

The authors thank Mr G. Lamorlette from Giat Industries, Head of the SAMPRASS project for his contribution in this aeroballistic study and for his encouragements.

## **REFERENCES**

1. N. BUSSIERE, "Essai de bagues aérofrein et tampons anti-ricochet pour munition de 155 Mle F1, le 14/10/93 à la Pointe", Note DGA/ETBS n° 76/93 du 30/11/1993.

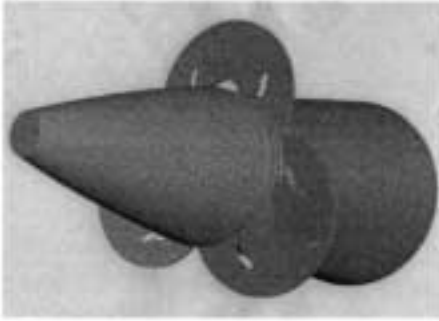


Fig 1: The SAMPRASS course-correction fuze.



Fig. 2: Principle of the correction.

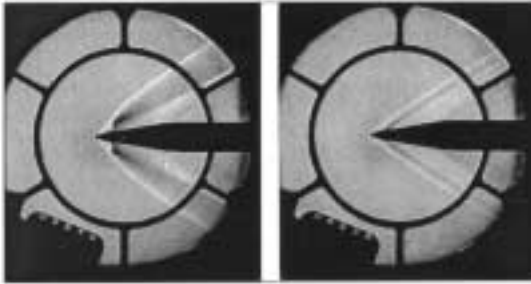


Fig 3 & 4: Schlieren visualizations with and without the correction fuze (S3MA wind tunnel).

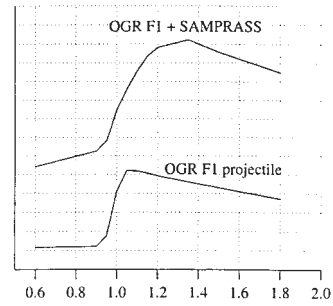


Fig. 5: Cxo versus the Mach number.

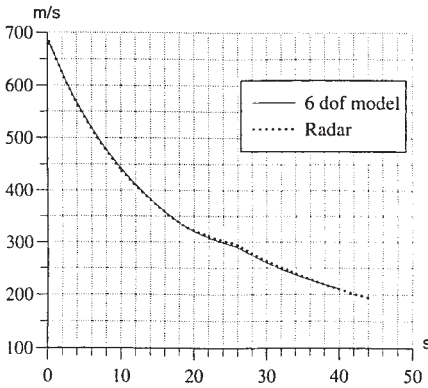


Fig. 6: Removal velocity measured by radar and determined by 6 dof simulation.

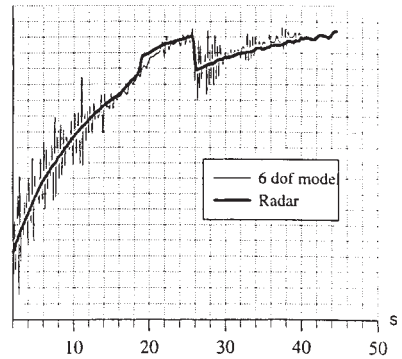


Fig. 7: Removal acceleration measured by radar and determined by 6 dof simulation.

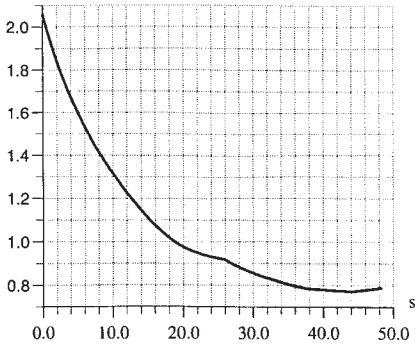


Fig. 8: Mach number during the flight versus time.

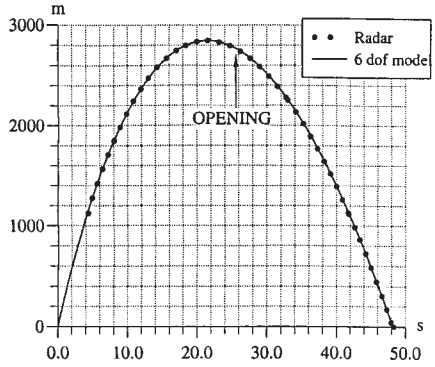


Fig. 9: Altitude of the projectile versus time.

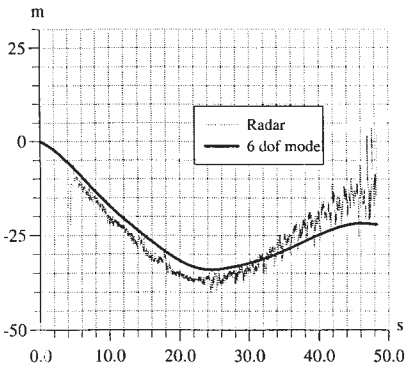


Fig. 10: Deviation of the projectile versus time (positive if right hand side deviation).

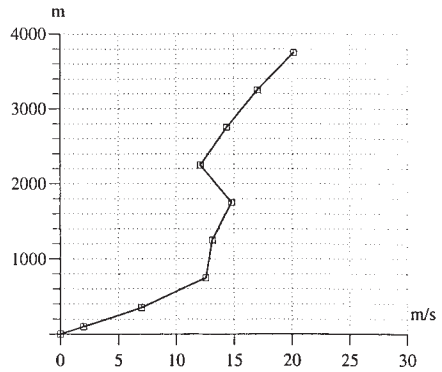


Fig. 11: Longitudinal wind versus altitude (rear wind if positive).

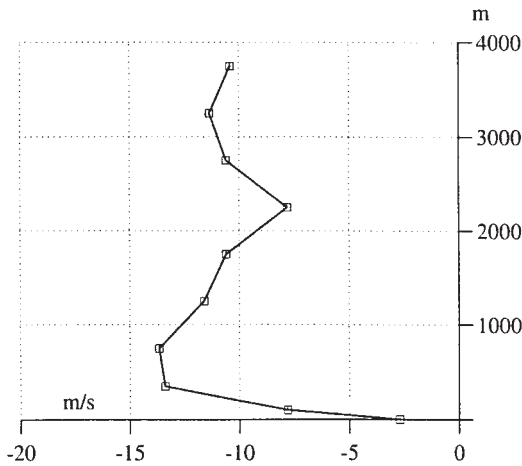


Fig. 12: Side wind versus time (negative if coming from the right).



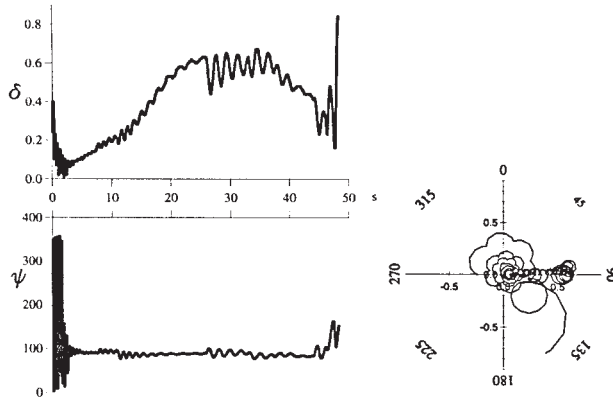


Fig. 13: Angular motion in fight conditions versus time (with measured aerology).

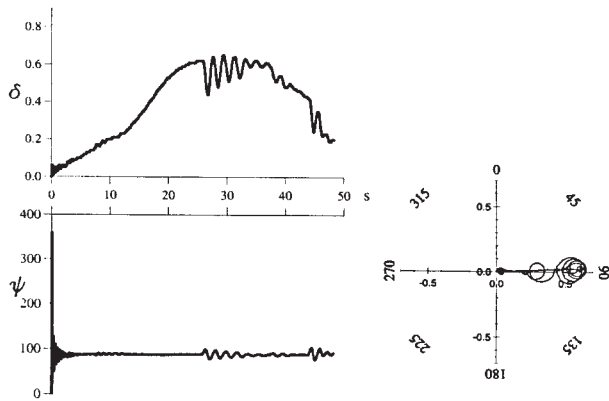


Fig. 14: Angular motion without wind versus time.

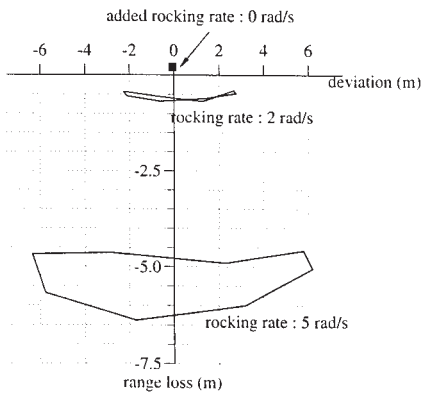


Fig. 15: Influence of the rocking rate due to the opening of airbrakes on the ground impact.

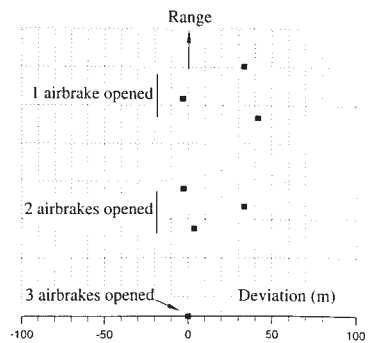


Fig. 16: Consequences of a partial opening of the airbrakes on the ground impact.

